

Title:

Topographic specificity of alpha power during auditory spatial attention

Author name and affiliation:

Yuqi Deng^{1*}, Inyong Choi², Barbara Shinn-Cunningham^{1,3}

*Corresponding author

¹ Department of Biomedical Engineering, Boston University, Boston, MA, USA, 02215

² Department of Communication Sciences and Disorders, University of Iowa, Iowa City, IA, 52242

³ Carnegie Mellon Neuroscience Institute, Carnegie Mellon University, Pittsburgh, PA 15213

Correspondence should be addressed to: Yuqi Deng, 610 Commonwealth Ave, 907, Boston, MA, 02215. E-mail: vydeng@bu.edu

The authors declare no financial conflicts of interest.

1 Abstract

2 Visual and somatosensory spatial attention both induce parietal alpha (7-14 Hz) oscillations whose
3 topographical distribution depends on the direction of spatial attentional focus. In the auditory
4 domain, contrasts of parietal alpha power for leftward and rightward attention reveal a qualitatively
5 similar lateralization; however, it is not clear whether alpha lateralization changes monotonically
6 with the direction of auditory attention as it does for visual spatial attention. In addition, most
7 previous studies of alpha oscillation did not consider subject-specific differences in alpha
8 frequency, but simply analyzed power in a fixed spectral band. Here, we recorded
9 electroencephalography in human subjects when they directed attention to one of five azimuthal
10 locations. After a cue indicating the direction of an upcoming target sequence of spoken syllables
11 (yet before the target began), alpha power changed in a task specific manner. Subject-specific peak
12 alpha frequencies differed consistently between frontocentral electrodes and parieto-occipital
13 electrodes, suggesting multiple neural generators of task-related alpha. Parieto-occipital alpha
14 increased over the hemisphere ipsilateral to attentional focus compared to the contralateral
15 hemisphere, and changed systematically as the direction of attention shifted from far left to far
16 right. These results showing that parietal alpha lateralization changes smoothly with the direction
17 of auditory attention as in visual spatial attention provide further support to the growing evidence
18 that the frontoparietal attention network is supramodal.

19 **Keywords:** electroencephalography, selective attention, human behavior, parietal cortex

20 **1 Introduction**

21 Visual spatial attention engages a well-studied frontoparietal network (e.g., Capotosto et al., 2009;
22 Corbetta, 1998; He et al., 2007; Shulman et al., 2010). This network involves distinct regions in
23 lateral frontal cortex that are separated by areas biased towards processing auditory inputs
24 (Michalka et al., 2016; Noyce et al., 2017). The visual attention network also includes a series of
25 retinotopic maps that start near primary visual sensory cortex and ascend along intraparietal sulcus
26 (IPS; e.g., see Sereno et al., 2001; Swisher et al., 2007). Activity in these retinotopic maps, which
27 represent contralateral space, is modulated by visual spatial attention; indeed, spatial attention
28 alone can lead to activation in these areas, even in the absence of visual stimulation (Saygin and
29 Sereno, 2008; Silver et al., 2005).

30 Many have argued that the frontoparietal network is supramodal, involved not just in visual spatial
31 attention, but also in somatosensory and auditory spatial attention. Recent fMRI evidence supports
32 this view. Specifically, auditory tasks involving spatial attention and spatial working memory
33 engage the same lateral frontal cortex regions active during visual tasks (Michalka et al., 2016;
34 Noyce et al., 2017). Auditory spatial tasks, but not non-spatial tasks, engage IPS (e.g., Alain et al.,
35 2001; Arnott et al., 2004), although this activation seems to be restricted to later, higher-order
36 maps without engaging the earlier IPS maps nearer to visual cortex (Michalka et al., 2016).

37 Neuroelectric imaging studies (using electro- and magnetoencephalography—EEG and MEG)
38 reveal a strong signature of the direction of visual spatial attention, attributed to activity in the
39 retinotopic IPS regions. When attention is directed to one side of space, there is typically an
40 increase in neural oscillation power in the alpha range (7-14 Hz) from ipsilateral parietal cortex,
41 and a decrease in alpha power from contralateral parietal cortex (Kelly et al., 2006; Thut et al.,
42 2006; Worden et al., 2000; Wöstmann et al., 2016). This lateralization of parietal alpha power

43 varies smoothly as the direction of visual spatial attention shifts, providing a readout of the
44 direction of visual attentional focus (Foster et al., 2016; Rihs et al., 2007; Samaha et al., 2016;
45 Worden et al., 2000). Given that parietal lobes primarily encode information about events that are
46 in contralateral exocentric space, parietal alpha lateralization is thought to reflect a suppression of
47 information (Foxe and Snyder, 2011; Klimesch, 2012; Klimesch et al., 2007; Romei et al., 2010).
48 Specifically, in the parietal lobe ipsilateral to the direction of attention, alpha increases to suppress
49 objects that are to be ignored, while in the parietal lobe contralateral to the direction of attention,
50 alpha decreases to allow processing of an attended object (Ikkai et al., 2016).

51 A few studies have contrasted parietal alpha lateralization when *auditory* spatial attention is
52 directed to the left versus to the right, and found a pattern that is qualitatively similar to that seen
53 in visual spatial attention (Klatt et al., 2018; Tune et al., 2018). Yet, there is little known about
54 whether auditory spatial attention varies monotonically as attentional focus shifts, as it does in
55 vision (Rihs et al., 2007; Samaha et al., 2015; van Gerven and Jensen, 2009; Worden et al., 2000).

56 To study the effects of spatial auditory attention on alpha activity, we designed an auditory
57 attention task in which listeners were cued at the start of each trial as to which of five spatial
58 locations (varying in lateral position) would contain a target sequence. We measured EEG as while
59 listeners were actively engaged in the auditory spatial attention task. We investigated how the
60 alpha peak frequency varied across the scalp, and how each subject's individualized parietal alpha
61 frequency power distribution was modulated by the direction of attention. One challenge in
62 studying alpha is that there may be significant differences across subjects in the alpha peak
63 frequency, as well as multiple generators of alpha, which also might vary in their peak frequency
64 as well as their topography on the scalp (Haegens et al., 2014). To enhance the sensitivity of our
65 analysis, we therefore determined subject-specific estimates of parietal alpha frequency and

66 analyzed how a narrow, 2 Hz wide band of power centered on this peak was modulated by the
67 direction of attention (as opposed to analyzing the average power over the range of observed alpha,
68 e.g., 7-14 Hz).

69 **2 Materials and Methods**

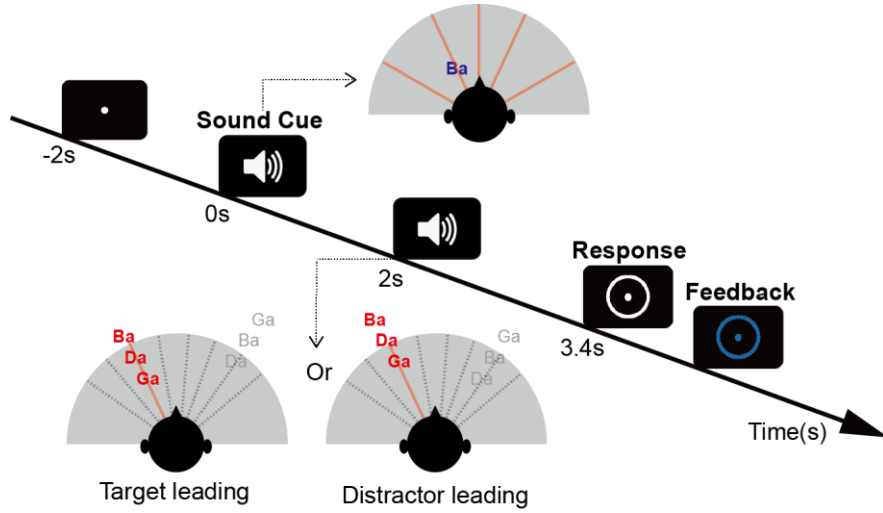
70 *2.1 Participants*

71 Thirty subjects (14 females, 18-30 years of age) participated in this study. All subjects had normal
72 hearing (hearing thresholds better than 20dB at pure tone frequencies between 250 Hz and 8 kHz).
73 All gave informed consent as approved by the Boston University Institutional Review Board. Two
74 subjects were excluded from the study due to an inability to perform the task (percentage of correct
75 responses equaled chance level). Subjects were asked to fill out an Edinburgh handedness
76 inventory questionnaire (Oldfield, 1971) to determine their handedness preference. Fourteen out
77 of the 28 remaining subjects were right-handed while the rest were left-handed.

78 *2.2 Paradigm*

79 Participants performed a spatial attention task in which they had to identify a target sequence of
80 three spoken syllables from one direction while ignoring a distractor sequence of three similar
81 syllables from another direction (Figure 1). At the start of each trial, a visual fixation dot appeared
82 on the screen. Two seconds later, an auditory cue was played from one of five possible locations
83 to indicate the spatial location of the upcoming target sequence. The target sequence and distractor
84 sequence onsets were separated by 200 ms, allowing the neural responses elicited by the onsets of
85 syllables in each stream to be temporally resolved. Within each stream, the syllable onsets were
86 separated by 500 ms. To make sure that listeners engaged spatial attention (rather than being able
87 to rely on temporal expectations), on half of the trials, the target stream began before the distractor,

88 while in the other trials the distractor began first. The first (target or distractor) sequence began to
89 play two seconds after the auditory cue.



90
91 *Figure 1. Trial design. A fixation dot appears at the center of the screen to instruct the*
92 *listeners to fixate their gaze. An auditory cue of 400ms duration (the spoken syllable /ba/)*
93 *begins 2 s later (at time zero) from one of five spatial locations chosen pseudo-randomly on*
94 *each trial, indicating the location from which the target will be presented (in the top inset*
95 *diagram, the /ba/ cue, in blue, is shown as coming from roughly 45 deg to the left, while the*
96 *five potential target directions are shown by red radial lines). After a preparatory period (0 s*
97 *- 2 s), two sound streams made up of random sequences of /ba/, /da/ & /ga/ (spoken by the*
98 *same talker) are presented. The target stream (colored red) appears from the cued direction*
99 *while a distractor stream (colored grey) appears from a different randomly chosen direction.*
100 *In each trial, the stream beginning first is selected randomly, and the other stream begins 200*
101 *ms later (in the bottom inset diagrams, the target begins first for the left example, but second*
102 *in the right example, while the distractor is presented from a location to the right; potential*
103 *distractor locations are shown by gray dashed lines). After the two streams finish playing (3.4*
104 *s after the sound cue is presented), a white circle appears on the screen, indicating that it is*

105 *time to report the target sequence. Immediately after the response is given, the circle changes*
106 *color to provide feedback (blue to indicate a correct response or red to indicate an incorrect*
107 *response).*

108 A circle appeared around the fixation dot 3.4 s after the sound cue (after both target and distractor
109 sequences finished playing), indicating the period during which subjects could record their
110 responses. After entering their response, the fixation dot and response circle changed color to
111 indicate whether the subject correctly reported the three target syllables (blue circle), or
112 misidentified one or more syllables (red circle).

113 Participants performed 12 statistically identical blocks, each made up of 40 trials (for a total of
114 480 trials per subject). The order of the trials within each block was random, with the constraint
115 that each of the five target locations was presented an equal number of times (each 8 times per
116 block). Thus, over the course of the 12 blocks, each subject performed 96 trials with the same
117 target location.

118 The syllables /ba/, /da/, & /ga/, spoken by the same female talker, were used both for both the
119 auditory cue and to make up the target and distractor streams. The auditory cue was a single
120 presentation of syllable (/ba/) with the spatial attributes of the upcoming target. The three-syllable
121 target and distractor sequences consisted of random sequences of the syllables, chosen with
122 replacement, and chosen independently for the target and distractor on each trial. All syllables
123 were presented over headphones at a sound level of 70 dB SPL.

124 We varied the interaural time difference (ITD) of the stimuli to manipulate their perceived lateral
125 position. Target sequences had ITDs of -600, -250, 0, 250, or 600 μ s (roughly corresponding
126 angular locations of -60°, -25°, 0°, 25°, 60°; Wightman and Kistler, 1992; Smith and Price, 2014).

127 On each trial, the distractor stream ITD was chosen to have an ITD that differed from the target
128 ITD by one of 8 increments (-600, -450, -300, -150, 150, 300, 450, 600 μ s), subject to the constraint
129 that the absolute value of the resulting ITD value never equaled or exceeded the ethological range
130 (max ITD magnitude of 700 μ s; Feddersen et al., 1957; Kuhn, 1977). For example, if the target
131 ITD was far to the right (target ITD: +600 μ s), the distractor ITD was chosen from the set 0, 150,
132 300, or 450 μ s (there were no possible ITDs farther to the right); if the target ITD was to the mid
133 left (target ITD: -250 μ s, as in Figure 1), then the distractor ITD was set to either -550 or -400 μ s
134 (to the left of the target) or -100, 50, 200, 350 or 500 μ s (to the right of the target). This restriction
135 was imposed to ensure that none of the trials was too easy, with very large separations between
136 the target and the distractor.

137 *2.3 Behavioral analysis*

138 We calculated the percentage of correctly recalled syllables for each one of the three syllables in
139 the target stream. For each of the syllables, we separately analyzed data from each of the 5 possible
140 target locations, broken down based on whether the target or the distractor stream was temporally
141 leading. Data were collapsed across the different distractor locations.

142 *2.4 EEG analysis*

143 *2.4.1 EEG data acquisition and preprocessing*

144 EEG data was recorded with 64-channel Biosemi ActiveTwo system in an Eckel sound treated
145 booth while participants performed the tasks. Two additional reference electrodes were placed on
146 the mastoids. The stimulus timing was controlled by Matlab (Mathworks, Natick, MA) using the
147 Psychtoolbox 3 extension (Brainard, 1997). EEG analyses included plotting scalp topographies

148 using the EEGLab toolbox (Delorme and Makeig, 2004) and performing other functions in the
149 Fieldtrip toolbox (Oostenveld et al., 2011).

150 EEG data from the correct trials were referenced against the average of the mastoid channels and
151 down-sampled to 256 Hz. EEG data was then epoched from the sound cue onset to the end of the
152 presentation period. Each epoch was baseline corrected by subtracting the mean from the baseline
153 period (the 100 ms prior to the auditory cue). After baseline correction, trials with a maximum
154 absolute value over 80 microvolts were rejected to remove artifacts (Delorme et al., 2007). Two
155 subjects with excessive artifacts were removed from further EEG analysis (less than 60% trials
156 remaining in at least one condition after artifact rejection). For the remaining 26 subjects, there
157 were at least 92 trials remaining for each condition after artifact rejection. To equate the number
158 of trials, 92 trials were randomly sampled for each condition for each subject for all subsequent
159 analysis.

160 2.4.2 Analysis of peak alpha power in frontocentral and parieto-occipital electrodes
161 For each epoch, the power spectrum was calculated over the 1s long period before the stimulus
162 onset, thereby avoiding inclusion of any strong evoked activity. Data segments were zero padded
163 to achieve a resolution of 0.1 Hz. For each subject and condition, the power spectra were averaged
164 across trials (96 trials per condition) to estimate the spectrum for each EEG channel.

165 We were interested in whether peak alpha frequency varied systematically across the scalp. To
166 assess this, we divided electrodes into frontal, frontocentral, and parieto-occipital groups based on
167 their locations on the scalp (see Figure 3A). The across-trial average power spectra were then
168 averaged across electrodes within each electrode group. The peak alpha frequency in each
169 electrode group was found by determining the local maxima of the average power spectra within

170 the 7-14 Hz band. If there were multiple peaks within this alpha range, the peak with the maximum
171 height was selected.

172 For more than half of the subjects, there was no clear alpha peak in the frontal electrode group.
173 Therefore, the frontal electrode group was excluded from this and any further alpha analysis.
174 Similarly, any subject for whom the alpha peak could not be detected in at least one of the
175 conditions for either frontocentral or parieto-occipital groups was excluded from further alpha
176 analysis. One left-handed subject was excluded for this reason.

177 2.4.3 Analysis of individualized parieto-occipital alpha frequency power
178 We wished to analyze how individual parieto-occipital alpha power changed with the spatial focus
179 of auditory attention. For all subjects with identifiable peak alpha frequencies, we defined the
180 individual parieto-occipital alpha frequency (IPAF) in the parieto-occipital electrode group. The
181 IPAF was calculated by averaging the EEG power spectra across all trials in all conditions and
182 across all parieto-occipital electrodes, then finding the peak frequency.

183 Once the IPAF was determined for each subject, we filtered all of their EEG data across the whole
184 scalp with a 2 Hz wide bandpass FIR filter centered on the IPAF (IPAF \pm 1Hz). We applied a
185 Hilbert transform to the bandpass filtered data to extract the individualized alpha energy envelope,
186 and took the magnitude of the transformed data. For each electrode and target location, we
187 calculated the time course of the IPAF power for each trial and then averaged across trials to
188 estimate the individualized induced alpha power time course (Snyder and Large, 2005). We
189 baseline corrected the average IPAF power against 1s before the cue onset. The mean power
190 averaged over the baseline period was subtracted from the IPAF power at each electrode. The
191 resulting data was then divided by the standard deviation of the baseline period. We then calculated

192 spatial z-scores of IAPF power for each electrode on the scalp by subtracting the mean IAPF power
193 averaged across all electrodes and normalizing against the global field power (Murray et al., 2008;
194 Skrandies, 1990). For each target location, we calculated the time course of the average IAPF
195 power spatial z-scores.

196 To determine whether the direction of attention significantly altered the topographic distribution
197 of alpha power, we contrasted the two extreme conditions: when subjects attended the leftmost
198 target (target ITD: -600 μ s) and when they attended the rightmost target (target ITD: +600 μ s).
199 Using the FieldTrip toolbox with Matlab, we performed a group-level analysis of GFP normalized
200 IAPF power. For each subject, we computed the average of IAPF power over the whole trial for
201 each electrode (0-3.4 s) for the leftmost and the rightmost conditions, resulting in two scalp
202 topography plots for each subject. We then performed a spatial clustering analysis with FieldTrip
203 to find clusters of electrodes across which the GFP normalized IAPF power differed significantly
204 in these two topography plots. Multiple comparison was controlled by undertaking a Monte Carlo
205 permutation test with 1000 random iterations using Fieldtrip. The cluster-based control has a type
206 I error level of $\alpha = 0.05$. The resulting clusters were then used to define the set of electrodes to
207 combine for further analysis.

208 IAPF power time courses of all electrodes within each statistically significant cluster were
209 averaged to produce one IAPF power time course for each cluster. A temporal clustering analysis
210 was performed on the cluster-based time courses across the 5 target locations to test whether IAPF
211 power changed significantly with direction of attention. Each time course was divided into 200 ms
212 long time bins. A linear regression model was applied for each time bin (independent variable of
213 target direction, dependent variable of magnitude of normalized IAPF power). An ANOVA was
214 applied to the linear regression model and Bonferroni correction was performed to control for

215 multiple comparisons. This analysis identified time windows exhibiting significant variation in
216 IPAF power for different directions of attention.

217 **3 Results**

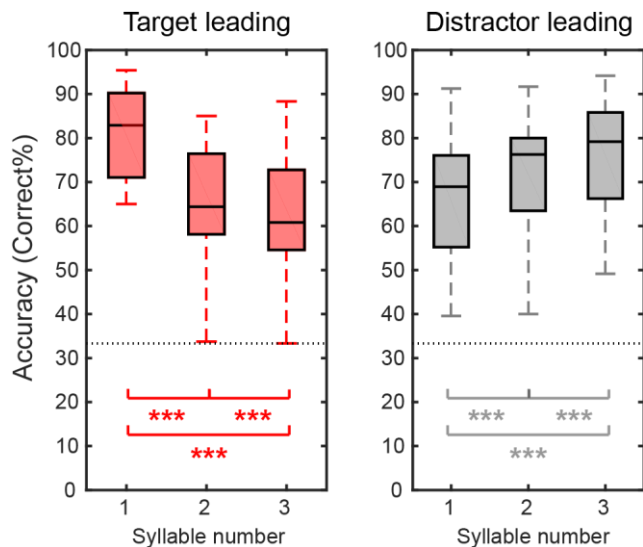
218 *3.1 Behavior*

219 Overall, participants were accurate in reporting the target sequence. All subjects were able to
220 perform significantly above chance level (33%).

221 We conducted an ANOVA to examine how the percentage of correct responses varied across
222 conditions. Given the sample size (N=28), we checked the normality of the sample distributions
223 using the Lilliefors normality test and found that all distributions passed ($P>0.05$) before
224 performing parametric statistical tests. The multi-way ANOVA had main factors of target location
225 (five ITDs), leading stream (target or distractor), and syllable temporal position (first, second, or
226 third). There was no main effect of target location [$F_{(4,839)}=1.14, P=0.34$] or of leading stream
227 [$F_{(1,839)}=2.41, P=0.12$]. Furthermore, there was no significant interaction between target location
228 and either of the other factors [target location \times leading stream: $F_{(4,839)}=1.22, P=0.30$; target
229 location \times syllable position: $F_{(8,839)}=0.22, P=0.99$], indicating that task performance did not vary
230 with target location. However, there was a significant main effect of syllable position [$F_{(2,839)}=11.1$,
231 $P<0.001$] and a significant interaction between syllable position and leading stream [$F_{(2,839)}=63.9$,
232 $P<0.001$].

233 Figure 2 shows the percentage of correctly recalling each syllable in the target leading (left panel)
234 and distractor leading (right panel) conditions (collapsing across target location). The data show
235 that when the target leads, performance decreases from the first target syllable to the last target
236 syllable, while this pattern reverses when the target lags.

237 To test the significance of these observations, we did post-hoc tests. We corrected for multiple
238 comparisons by calculating post-hoc test statistics using the Benjamini-Hochberg FDR correction
239 (Benjamini and Hochberg, 1995). Our post hoc tests (paired t-tests) showed that the percentage of
240 correct response decreases systematically with syllable number when the target stream leads
241 (syllables 1 vs. 2, $t_{(27)}=9.83, P<0.001$; syllables 1 vs. 3, $t_{(27)}=9.49, P<0.001$; syllables 2 vs. 3,
242 $t_{(27)}=3.78, P<0.001$), but performance improves from syllable to syllable when the distractor
243 stream leads; (syllables 1 vs. 2, $t_{(27)}=4.94, P<0.001$; syllables 1 vs. 3, $t_{(27)}=6.99, P<0.001$; syllables
244 2 vs. 3, $t_{(27)}=3.80, P<0.001$).



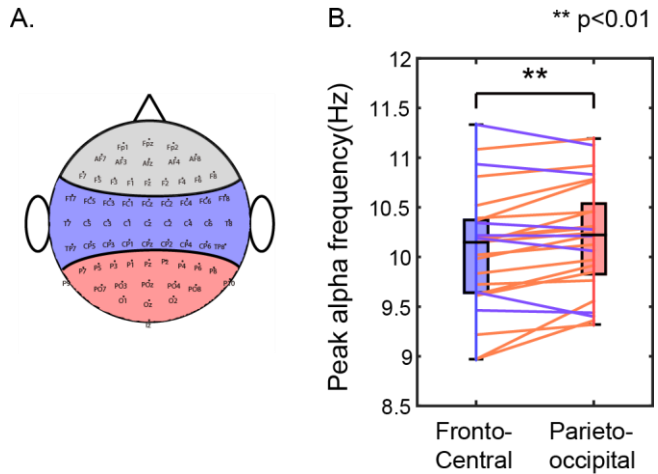
245
246 *Figure 2. Behavioral performance averaged across subjects for the target leading (left panel)*
247 *and distractor leading (right panel) conditions. Within each panel, we show boxplots of*
248 *percent correct responses (central black line shows the across-subject mean; boxes show the*
249 *25th – 75th percentile ranges; error bars show the range from minimum to maximum) for each*
250 *syllable position within the target stream. The horizontal gray dashed line shows chance*
251 *performance (33%). Asterisks indicate percentages that differ significantly from one another*
252 *based on post hoc tests (* $p<0.05$; ** $p<0.01$; *** $p<0.001$).*

253 We tested whether handedness influenced behavioral performance using a two-sample t-test at the
254 group level. We found no significant difference between left-handed and right-handed groups'
255 performance [$t_{(14)}=0.53, P=0.60$].

256 *3.2 Peak alpha power in frontocentral and parieto-occipital electrodes*

257 For each subject and target location, we computed the frequency that had the greatest average
258 power within the alpha range separately for frontocentral electrodes and parieto-occipital
259 electrodes. These results, shown in Figure 3, suggest that alpha peak frequency is higher in parieto-
260 occipital electrodes than in frontocentral electrodes.

261 We explored the statistical significance of these observations by conducting a multi-way repeated-
262 measure ANOVA on peak alpha frequency with main factors of electrode group (frontocentral and
263 parieto-occipital) and target location (five ITD values). There was no significant main effect of
264 target location on alpha peak frequency [$F_{(4,249)}=1.63, P=0.12$] and no significant interaction
265 between target location and electrode group [$F_{(4,249)}=0.80, P=0.53$]. However, there were
266 significant main effects of both subject identity [$F_{(24,249)}=220, P<0.001$] and electrode group
267 [$F_{(1,249)}=59.27, P<0.001$], as well as significant interactions of subject identity with both electrode
268 group [$F_{(24,249)}=6.61, P<0.001$] and target location [$F_{(96,249)}=1.51, P=0.022$]. These results suggest
269 that while peak alpha frequency varies across subjects, there is a consistent difference in the peak
270 alpha frequency in frontocentral and parieto-occipital electrodes. Post-hoc t-test reveals that the
271 alpha peak frequency is generally higher in the parieto-occipital region than in the frontocentral
272 region [$t_{(24)}=2.99, P=0.006$; paired t-test; Figure 3B].



273

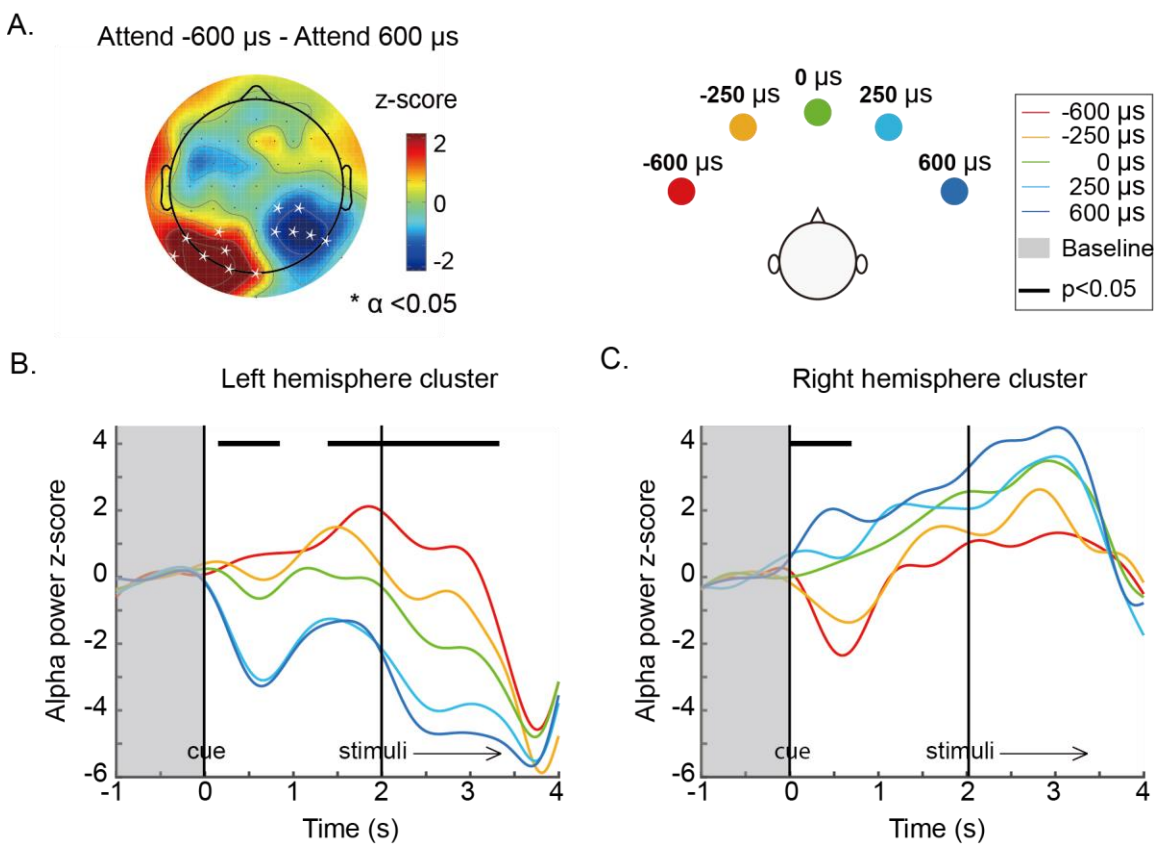
274 *Figure 3. Peak alpha power is greater in parieto-occipital electrodes compared to*
275 *frontocentral electrodes. A. Definition of electrode groups. Blue and red area represents the*
276 *electrodes included in frontocentral and parieto-occipital groups; frontal electrodes (in gray)*
277 *showed less consistent and robust alpha, and therefore were not analyzed. B. Comparison of*
278 *peak alpha frequency in the frontocentral and parieto-occipital electrodes. Box plots show*
279 *group comparisons (as in Figure 2). Blue and red colored dots plot results from individual*
280 *subjects; colored lines connect peak frequencies in the two electrode groups for a given*
281 *subject, with the color of the connecting line shows which peak frequency is greater: blue*
282 *lines indicate higher peak frequency in frontocentral electrodes, while red lines indicate*
283 *higher peak frequency in parieto-occipital electrodes.*

284 We also conducted a group level two-sample t-test to examine whether alpha peak frequency
285 varied with handedness. We did not find any significant difference in peak alpha frequency
286 between the left-handed and the right-handed groups [$t_{(23)}=1.37, P=0.18$].

287 *3.3 Individualized parieto-occipital alpha frequency power*

288 We explored how the topographic distribution of individual parieto-occipital alpha frequency
289 power changed with the spatial focus of auditory attention. Figure 4A shows a scalp topography

290 plot of the difference, at each electrode, between the average IPAF power when attending far left
291 (target ITD: -600 μ s) and far right (target ITD: 600 μ s). Significant electrodes from spatial
292 clustering results are overlaid on the topography plot. A positive cluster was found on the left
293 parieto-occipital region ($P=0.007$) and a negative cluster was found on the right hemisphere
294 ($P=0.009$). This result is in consistency with the previous literature, which reports that alpha
295 oscillation power decreases in the hemisphere contralateral to an attended location and increases
296 in the hemisphere ipsilateral to an attended location (Banerjee et al., 2011; Kelly et al., 2006;
297 Klimesch, 2012; Worden et al., 2000).



299 *Figure 4. A. Topography of alpha power z-score difference between attend far left (target*
300 *ITD: -600 μ s) and attend far right (target ITD: 600 μ s) averaged over the whole trial (0-*
301 *3.4s). Channels within a cluster in which alpha power changes significantly with direction of*

302 *attention are marked by asterisks. B & C. Time courses of alpha power dynamics across the*
303 *trial period for the left parieto-occipital cluster and the right parieto-occipital cluster.*
304 *Individualized parieto-occipital alpha power was averaged within the left and right clusters*
305 *shown in A and plotted as a function of time for each target location. Data were divided into*
306 *200 ms long time bins and averaged within each time bin. Asterisks at the top of the plot*
307 *(forming continuous bars, visually) show the time windows in which there was a statistically*
308 *significant effect of target direction on alpha power after Bonferroni correction. Vertical*
309 *black lines illustrate the onsets of auditory cue and stimuli. Shadowed areas represent the*
310 *baseline period.*

311 To investigate the influence of handedness on alpha lateralization, we calculated the degree of
312 alpha lateralization for each subject in each attention condition. Specifically, for each target
313 direction, we subtracted the IPAF power averaged across the right hemisphere cluster (which is
314 generally negative for attention to the left and positive for attention to the right) from the IPAF
315 power averaged across the left hemisphere cluster (which is generally positive for attention to the
316 left and negative for attention to the right). ANOVA revealed a significant main effect of target
317 location on lateralization ($F_{(4,129)}=7.33, P<0.001$) but no significant effect of handedness
318 ($F_{(2,129)}=2.68, P=0.10$) and no significant interaction between handedness and attention focus
319 ($F_{(4,129)}=0.08, P=0.99$).

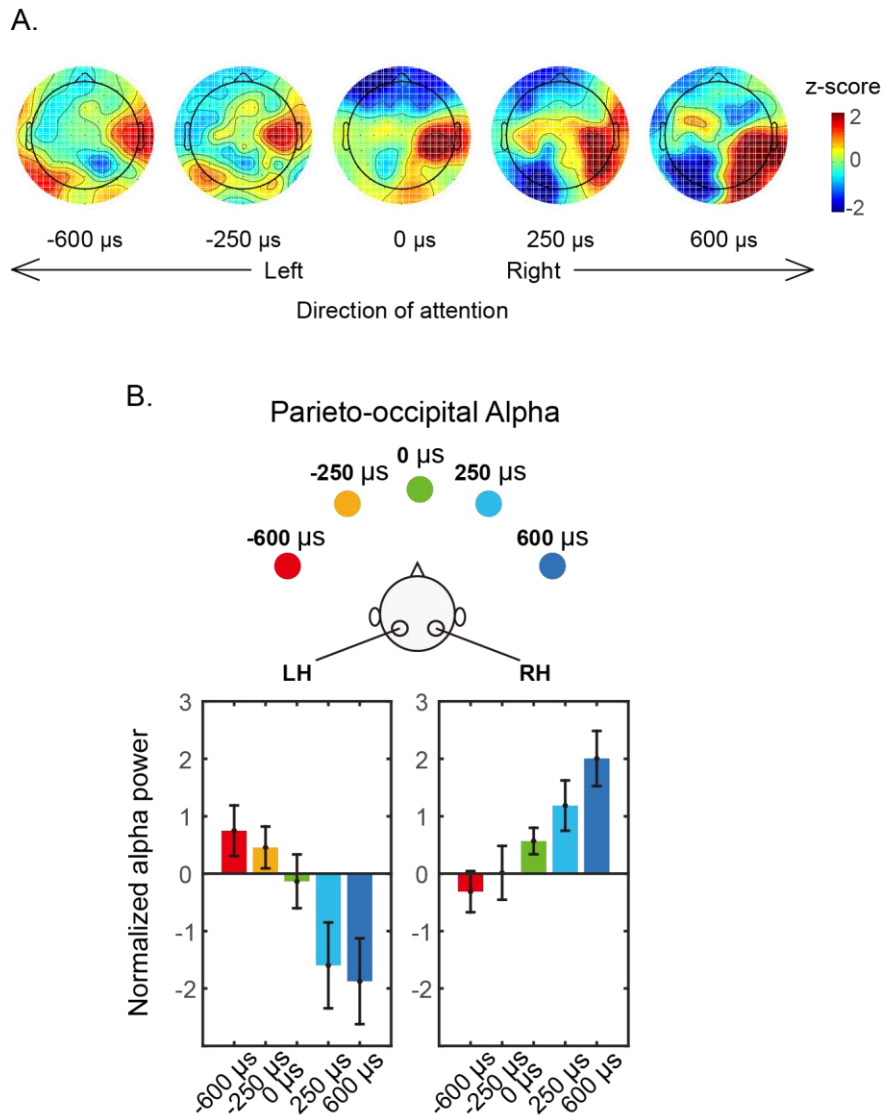
320 Within each cluster, the average was taken to render the time courses of IPAF power in each
321 attention focus condition (Figure 4B & 4C). The IPAF power time courses reveal that alpha power
322 increases systematically as the focus of spatial attention shifts from left to right in the left parieto-
323 occipital cluster, and decreases systematically in the right parieto-occipital cluster.

324 To test for the significance of these effects, we performed a linear regression analysis for each 200
325 ms long time bin. Bonferroni corrected results revealed that alpha power varies significantly with
326 direction of attention in a number of time periods. In the left parieto-occipital cluster, alpha power
327 changed significantly with target direction immediately after the cue (0.2-0.8s) and again from
328 right before the target/distractor sound began until it finished played (1.6-3.2s; Figure 4B). The
329 opposite trend is seen throughout the trial in the right parieto-occipital cluster; however, this
330 variation was only statistically significant immediately after the cue appeared (0-0.8s; Figure 4C).

331 Given that both left and right parieto-occipital clusters show significant differences in alpha power
332 during the preparatory period, we undertook a final analysis to quantify how alpha power varied
333 across the scalp with direction of attentional focus. To this end, for each electrode we averaged
334 alpha power in the preparation period (0s – 2s, after the onset of the cue for where to attend, but
335 before the onset of the target and distractor stimuli) for each target location.

336 Figure 5A shows these average alpha power values across the scalp. As attentional focus shifts
337 from left to right, there is a clear change in the power of alpha in parieto-occipital electrodes: alpha
338 decreases systematically in the left parieto-occipital electrodes and increases systematically in the
339 right parieto-occipital electrodes. To visualize these changes, we took the average alpha power
340 over the left and right parieto-occipital clusters identified above (see Figure 4A), and plotted the
341 mean activity as a function of target ITD (Figure 5B). These results show that in left parieto-
342 occipital electrodes, alpha power is significantly greater than baseline when attention is directed
343 ipsilaterally (far left of the left panel of Figure 5B); decreases as attention shifts to contralateral,
344 right exocentric space (moving from left to right in the panel); and is significantly below baseline
345 (reduced alpha) when attention is focused on the right. Consistent with past work on parieto-
346 occipital responses during attention, our results are not symmetric (Haegens et al., 2011; Ikai et

347 al., 2016). In the right parieto-occipital cluster, alpha power is greater than baseline when attention
348 is directed ipsilaterally (far right of the right panel of Figure 5B); decreases as attention shifts to
349 contralateral, left exocentric space (moving from right to left in the panel); but never falls
350 significantly below baseline, even when attention is focused on the far left.



351
352 *Figure 5. Parieto-occipital alpha power during the attentional preparatory period (-2 to 0s).*
353 *A. Topographies of alpha power z-scores for the five different target locations. B. Parieto-*

354 *occipital alpha averaged within the left and right parieto-occipital clusters revealed by*
355 *clustering analysis.*

356 **4 Discussion**

357 We tested subjects engaged in a challenging auditory spatial attention task and observed how alpha
358 oscillation power changed during task performance. Importantly, the task was designed to require
359 sustained auditory spatial attention: two competing streams, each a sequence of three syllables
360 selected from the same set of tokens, spoken by the same talker, and overlapping in their time of
361 presentation, were presented with two different ITDs. Subjects were asked to report the target
362 sequence from the direction indicated by an auditory cue at the start of each trial, while ignoring
363 the distractor (from an unknown direction). In order to force listeners to rely on spatial cues, which
364 of the streams began first was random from trial to trial, and counter balanced.

365 Behaviorally, listeners were good on the task. Still, the pattern of behavioral results depended on
366 the exact stimulus configuration. Specifically, when the target began before the distractor, listeners
367 were very good at reporting the first target syllable; however, they were worse at reporting the
368 second, and even worse at reporting the third. Given that the distractor began playing before the
369 second syllable, this decrease in performance with syllable number is not very surprising, and
370 likely reflects a combination of both energetic masking (e.g., see Arbogast et al., 2002; Brungart,
371 2001) and more central, cognitive interference (e.g., see Shinn-Cunningham, 2008). The opposite
372 pattern occurs when the distractor began first: performance was worst for the first syllable, better
373 for the middle syllable, and best for the final syllable. Again, this pattern makes sense. The sudden
374 onset of the distractor at the start of the presentation undoubtedly grabs attention involuntarily
375 (see, for example, Buschman and Miller, 2007; Conway et al., 2001; Elhilali et al., 2009). The first
376 target syllable begins only 200 ms after the distractor; this brief delay is close to the limit for how

377 quickly listeners can shift attention away from the salient distractor onset, which impacts the ability
378 to report the first target syllable. Over time, spatial attention to the correct stream builds up, leading
379 to better focus as the presentation continues, consistent with some previous studies of auditory
380 attention (Best et al., 2008; Dai et al., 2018). Moreover, the distractor sequence ends before the
381 third target syllable begins. Together, these effects lead to improvement in performance from
382 syllable to syllable on trials where the distractor begins first. Overall, however, it is clear that
383 listeners were able to perform the task well, and that they relied on auditory spatial cues to perform
384 the task.

385 *4.1 There are significant subject differences in alpha peak frequency*

386 We observed that alpha peak frequency varied across individuals, consistent with previous reports
387 (Basar, 2012; Bodenmann et al., 2009; Klimesch, 1999). For instance, we found that during the
388 task, the peak alpha frequency in individual listeners' parieto-occipital electrodes ranged from 9-
389 11.3 Hz (standard deviation of 0.6 Hz). This observation argues for the importance of analyzing
390 alpha in subject-specific ways (Haegens et al., 2014). We therefore estimated the alpha peak
391 frequency for each subject and used this to estimate alpha power in all subsequent analysis. Using
392 subject-specific analysis of alpha ensures that we get the cleanest, most robust measures of how
393 alpha power changes with task demands.

394 *4.2 Multiple generators of alpha are engaged during selective auditory spatial attention*

395 We separately analyzed the dominant frequency of alpha power in frontal, frontocentral, and
396 parieto-occipital electrodes. While there was not a robust peak in alpha power in frontal electrodes,
397 we found clear peaks in frontocentral and parieto-occipital sensors. Moreover, we found consistent
398 differences in the frequency of the dominant alpha peak in frontocentral versus parieto-occipital
399 electrodes. Specifically, the peak frequency of alpha in the frontocentral electrodes is significantly

400 lower than in the parieto-occipital electrodes: 19 out of 25 subjects showed peak frequencies of
401 frontocentral alpha that were lower than for parieto-occipital alpha (see Figure 3). This difference
402 in alpha peak frequency provides strong evidence for multiple generators of alpha activity during
403 auditory tasks, leading to different scalp topographies (one stronger over frontocentral electrodes
404 and one stronger over parieto-occipital electrodes).

405 A number of previous studies have reported changes in alpha oscillation power during challenging
406 auditory tasks. However, different studies attribute different roles to these oscillations and what
407 they signify. For instance, previous studies have reported that during auditory spatial attention,
408 alpha activity tends to lateralize, increasing ipsilateral to the direction of attention and decreasing
409 contralateral to the direction of attention in both temporal (e.g., Hartmann et al., 2012) and
410 posterior brain regions (e.g., Banerjee et al., 2011; Wöstmann et al., 2016). Increases in alpha
411 power have been associated with increases in cognitive load in temporal as well as posterior
412 portions of the brain (Van Dijk et al., 2010; Wilsch and Obleser, 2016; Woestmann et al., 2017),
413 and alpha power increases with listening effort (Woestmann et al., 2015). Prestimulus alpha has
414 been shown to reflect decision processes (Woestmann et al., 2019). The current study is consistent
415 with the various reports of alpha power reflecting a range different functions during auditory task
416 performance; our results suggest that during our auditory spatial attention there are multiple
417 generators of alpha, which come from different neural regions and thus reflect different cognitive
418 processes (see also Weisz et al., 2014). Indeed, the point that multiple alpha generators likely
419 contribute during different auditory tasks has been put forth in a recent review paper (Strauß et al.,
420 2014).

421 Some previous studies have shown that in addition to affecting alpha power, task engagement and
422 even task load can influence peak alpha frequency (e.g., Basar, 2012; Haegens et al., 2014). In the

423 current task, even though we expected to see (and saw) changes in parietal alpha power with the
424 direction of attention (see the discussion below), we did not find any changes in alpha peak
425 frequency when we varied target location. This result makes sense, given that task performance
426 (and thus task difficulty) was similar for different target locations. Our results are consistent with
427 the idea that, regardless of the specific direction of attention (target location), the same brain
428 networks are engaged in performing the same basic cognitive functions during the task, which
429 leads to the same frequencies of alpha oscillations across all conditions.

430 Our study methods limit our ability to localize the generators of observed neural activity (EEG
431 measures with a small number of sensors and without any subject-specific models of anatomical
432 structure); thus, we cannot, from the current results, make strong claims of where the different
433 neural generators of alpha oscillations lie. Given how EEG signals propagate to the scalp, parietal
434 sources of alpha are likely to dominate the observed responses from parieto-occipital electrodes,
435 while sources more frontal sources likely dominate the responses in frontocentral electrodes.
436 Regardless, our results provide good evidence that there are at least two different generators of
437 alpha oscillations during our auditory task.

438 The alpha power we observe in frontocentral electrodes central alpha range oscillation could be a
439 mu rhythm, related to motor planning (Llanos et al., 2013; Sabate et al., 2012). The frequency
440 range of mu rhythms (7.5-12.5Hz) overlaps with alpha. In our task, the task-related modulation of
441 frontocentral alpha led to greater alpha power in right-hemisphere electrodes, but not in left-
442 hemisphere electrodes, and did not vary significantly with the direction of attention (consider
443 Figures 4A & 5A). This pattern is consistent with a right-handed motor response during the task,
444 which leads to an increase of mu oscillations over right motor cortex [related to suppression of
445 movement of the left hand; (Pfurtscheller et al., 2006, 2000; Wolpaw et al., 2002)]. While we

446 tested both right- and left-handed subjects, even left-handed subjects used the numeric keypad (on
447 the right side of a keyboard) to enter their responses, consistent with the observed results.
448 Alternatively, the more frontal alpha source could be from auditory sensory cortex, which has been
449 reported to generate alpha power that fluctuates during auditory task performance (Frey et al.,
450 2014).

451 Future work is needed to tease apart how different neural generators behave during tasks like that
452 used here. To address these questions, neuroimaging techniques with better spatial resolution
453 should be employed to allow localization of the underlying neural generators.

454 *4.3 Parieto-occipital alpha power topography reflects the lateral position of auditory spatial
455 attentional focus*

456 We found that when auditory attention is covertly oriented to a particular spatial location, alpha
457 power in parieto-occipital electrodes lateralizes, increasing in the electrodes ipsilateral to the
458 direction of attention and decreasing in the contralateral electrodes. These results are consistent
459 with previous studies of both visual and auditory spatial attention (Frey et al., 2014; Sauseng et
460 al., 2005; Strauß et al., 2014; Thut et al., 2006; Wöstmann et al., 2016). Our study extends these
461 previous findings by contrasting the topographic distribution of alpha power as a function of the
462 lateralization of attention, testing five different target directions ranging from far left to far right:
463 the farther lateralized the focus of attention focus, the greater the lateralization of parietal alpha
464 power. While previous studies have shown that it is possible to decode the focus of visual attention
465 from the distribution of alpha power (Foster et al., 2016; O’Sullivan et al., 2015; Rihs et al., 2007;
466 Samaha et al., 2017), the topographic distribution of alpha power has, to our knowledge, not been
467 shown previously to change systematically with the direction of auditory spatial attention. Previous
468 studies of auditory spatial attention have generally only considered how alpha is distributed during

469 attention to one location on the left versus attention to a symmetric location on the right, or even
470 for dichotic sounds (a sound presented only to the left ear and a different sound presented only to
471 the right ear).

472 The pattern of alpha lateralization that we report is consistent with the theory that alpha reflects a
473 suppressive or inhibitory mechanism (Jensen and Mazaheri, 2010; Klimesch, 2012; Klimesch et
474 al., 2007; Strauß et al., 2014). Specifically, parietal cortex has a contralateral bias, primarily
475 encoding information from contralateral exocentric space (Kaiser et al., 2000; Schonwiesner et al.,
476 2006; Teshiba et al., 2013). Given that spatial auditory processing engages retinotopically
477 organized parietal maps of contralateral space (Huang et al., 2014), increases in alpha power
478 ipsilateral to the direction of attention are consistent with suppressing interfering information about
479 events in the opposite direction. Attention to a particular retinotopic location is likely to cause an
480 alpha-linked suppression of information in subnetworks of the brain representing other retinotopic
481 locations. Our observation of a gradation of parietal alpha power lateralization that reflects the
482 exact attentional focus is consistent with the theory that local alpha power modulation “reflects
483 changes in the excitability of populations of neurons whose receptive fields match the locus of
484 attention” (Ikkai et al., 2016; Klimesch, 2012).

485 Visual attention studies show that the topography of parietal alpha varies not only with left-right
486 lateral angle, but also with elevation. Although perception of auditory elevation is substantially
487 less precise than perception of auditory lateral angle (which is already much less precise than visual
488 perception of angle), it would be interesting to explore whether changes in the elevation of auditory
489 spatial attention (e.g., using free-field speakers to provide rich, realistic auditory elevation cues)
490 also affect the distribution of parietal alpha power.

491 *4.4 Is the frontoparietal network truly a supramodal spatial attention network?*

492 As discussed above, we find that just like in both vision (e.g., Kelly et al., 2006; Worden et al.,
493 2000) and touch (e.g., S. Haegens et al., 2011), spatial attention directed to an auditory target
494 causes a shift in parietal alpha power (with relatively greater power in parieto-occipital electrodes
495 ipsilateral to the direction of attention; Banerjee et al., 2011; Wöstmann et al., 2016). Given the
496 difficult in localizing the sources of the observed EEG results, however, this alone provides
497 relatively weak support for the idea that the spatial attention network is shared between vision and
498 audition.

499 A couple of neuroelectric studies have directly contrasted parietal alpha lateralization for visual
500 and auditory spatial attention, and found clear differences in topography (Frey et al., 2014;
501 Banerjee et al., 2011). Indeed, in MEG, which provides better resolution of deeper brain structures
502 than does EEG (Frey et al., 2014), auditory spatial attention was shown to modulate the
503 lateralization of alpha in auditory sensory cortex, but not visual spatial attention. Yet, although
504 there were differences in alpha topography for visual and auditory spatial attention tasks, alpha
505 lateralization in parieto-occipital regions was similar across modalities. Thus, while there are
506 multiple generators of alpha during auditory tasks, the alpha associated with suppression in parietal
507 cortex may well reflect the same cognitive mechanism during visual and auditory spatial attention.

508 Recent fMRI work that uses subject-specific definitions of regions of interest (ROIs) based on
509 functional localizers supports the view that auditory spatial processing engages the very same
510 regions that are always engaged during visual processing. Specifically, distinct frontal executive
511 control regions that are biased towards visual processing are differentially more engaged during
512 auditory attention and working memory tasks (Kong et al., 2014; Michalka et al., 2016; Noyce et
513 al., 2017). Importantly, these executive regions, together with retinotopically mapped regions in

514 parietal cortex, form a coherent network that is seen during fMRI resting state in both subject-
515 specific ROI analysis (Michalka et al., 2016) and that emerge at a group level from the large-scale
516 connectome dataset (Tobeyne et al., 2018). These results lend further support to the view that the
517 frontoparietal visual spatial attention network is also engaged during auditory spatial processing.

518 Another piece of evidence for the supramodal nature of parietal representations is the common
519 asymmetry seen in the information representation across modalities. The right hemisphere
520 dominance theory posits that the left hemisphere represents information from right exocentric
521 space, whereas the right hemisphere, while biased towards representing left exocentric space, also
522 represents ipsilateral information (Huang et al., 2014; Mesulam, 1999; Okazaki et al., 2015; Pouget
523 and Driver, 2000; Shulman et al., 2010). This asymmetry helps explain why hemifield neglect is
524 common for sources in left exocentric space (i.e., in patients with right lesions in parietal cortex
525 that destroys the only information about leftward sources), but uncommon for right exocentric
526 space (Heilman and Abell, 1980). This kind of left-right asymmetry is seen not only in past results,
527 but in our current auditory spatial attention data.

528 Specifically, previous neuroelectric studies in both vision (e.g., Ikkai et al., 2016) and touch (e.g.,
529 Haegens et al., 2011) report greater modulation of parietal alpha power when attention is directed
530 to left compared to right exocentric space. We see the same asymmetry. During the preparatory
531 period (following the cue but before the stimuli began), alpha power in the left electrode cluster
532 decreased below baseline when attention was focused on the right, and increased above baseline
533 when attention was focused on the left. In contrast, in right electrodes, preparatory alpha power
534 never decreased significantly below baseline, even when attention was directed to the far left.
535 Furthermore, attentional modulation of parietal alpha was significant throughout the presentation

536 of the target-distractor stimuli in left parieto-occipital electrodes, but less robust (and not
537 statistically significant) during the stimuli in right parieto-occipital electrodes.

538 We included equal numbers of left- and right-handed subjects in the study with the intention of
539 studying effects of atypical hemispheric asymmetry in left-handed subjects. However, we did not
540 find any significant difference between left- and right-handed subjects in any of our analyses. For
541 this reason, we collapsed all of our data across these groups in the presented results. Given the
542 number of subjects we were able to test, combined with the relatively low incidence of atypical
543 hemispheric dominance even in left-handed participants (Knecht, 2000), this failure to find an
544 effect is not particularly surprising. Future studies with a prescreening procedure to test for
545 hemispheric dominance, and separating participants into groups based on this independent
546 measure, would undoubtedly shed more light on how parietal processing is affected when subjects
547 have an atypical spatial representation (e.g., Cai et al., 2013).

548 **5 Conclusions**

549 We studied how individualized parietal alpha power shifts as a function of the lateral direction of
550 auditory spatial attention. We presented auditory targets from one of five azimuth locations by
551 varying ITD from -600 μ s to +600 μ s. We found unique alpha peak frequencies over frontocentral
552 and parieto-occipital electrodes, revealing the presence of at least two distinct generators of alpha
553 oscillations during our task. The parieto-occipital alpha power was modulated by the lateral focus
554 of attention, varying systematically with the focus of auditory attention. The similarity to previous
555 results from other sensory modalities in alpha power lateralization, down to an asymmetry between
556 alpha power changes in left versus right hemisphere, supports the view that the same cognitive
557 processes are engaged during spatial attention across sensory modalities. Past fMRI evidence that

558 the exact brain regions engaged by auditory spatial processing are part of the well-studied
559 frontoparietal visual processing network; together with current results, the current study supports
560 the idea that there is a common, supramodal spatial attention network.

561 **Acknowledgements**

562 This work was supported by the National Institutes of Health [NIDCD R01 DC013825].

563 **References**

564 Alain, C., Arnott, S.R., Hevenor, S., Graham, S., Grady, C.L., 2001. "What" and
565 "where" in the human auditory system. *Proc. Natl. Acad. Sci. USA* 98, 12301–
566 12306. <https://doi.org/10.1073/pnas.211209098>

567 Arbogast, T.L., Mason, C.R., Kidd, G., 2002. The effect of spatial separation on informational
568 and energetic masking of speech. *J. Acoust. Soc. Am.* 112, 2086–2098.
569 <https://doi.org/10.1121/1.1510141>

570 Arnott, S.R., Binns, M.A., Grady, C.L., Alain, C., 2004. Assessing the auditory dual-pathway
571 model in humans. *Neuroimage* 22, 401–408.
572 <https://doi.org/10.1016/j.neuroimage.2004.01.014>

573 Banerjee, S., Snyder, A.C., Molholm, S., Foxe, J.J., 2011. Oscillatory Alpha-Band Mechanisms
574 and the Deployment of Spatial Attention to Anticipated Auditory and Visual Target
575 Locations: Supramodal or Sensory-Specific Control Mechanisms? *J. Neurosci.* 31, 9923–
576 9932. <https://doi.org/10.1523/jneurosci.4660-10.2011>

577 Basar, E., 2012. A review of alpha activity in integrative brain function: Fundamental
578 physiology, sensory coding, cognition and pathology. *Int. J. Psychophysiol.* 86, 1–24.

579 Benjamini, Y., Hochberg, Y., 1995. Controlling the False Discovery Rate: A Practical and
580 Powerful Approach to Multiple Testing. *J. R. Stat. Soc. Ser. B* 57, 289–300.

581 <https://doi.org/10.1111/j.2517-6161.1995.tb02031.x>

582 Best, V., Ozmeral, E.J., Kopco, N., Shinn-Cunningham, B.G., 2008. Object continuity enhances
583 selective auditory attention. *Proc. Natl. Acad. Sci.* 105, 13174–13178.

584 <https://doi.org/10.1073/pnas.0803718105>

585 Bodenmann, S., Rusterholz, T., Jaggi-Schwarz, K., Durr, R., Bachmann, V., Landolt, H.-P.,
586 Stoll, C., Geissler, E., 2009. The Functional Val158Met Polymorphism of COMT Predicts
587 Interindividual Differences in Brain Oscillations in Young Men. *J. Neurosci.* 29, 10855–
588 10862. <https://doi.org/10.1523/JNEUROSCI.1427-09.2009>

589 Brainard, D.H., 1997. The psychophysics toolbox. *Spat. Vis.* 10, 433–436.

590 Brungart, D.S., 2001. Informational and energetic masking effects in the perception of two
591 simultaneous talkers. *J. Acoust. Soc. Am.* 109, 1101–1109.

592 <https://doi.org/10.1121/1.1345696>

593 Buschman, T.J., Miller, E.K., 2007. Top-Down Versus Bottom-Up Control of Attention in the
594 Prefrontal and. *Science* (80-.). 315, 1860–1863.

595 Cai, Q., Van der Haegen, L., Brysbaert, M., 2013. Complementary hemispheric specialization for
596 language production and visuospatial attention. *Proc. Natl. Acad. Sci.* 110, E322–E330.

597 <https://doi.org/10.1073/pnas.1212956110>

598 Capotosto, P., Babiloni, C., Romani, G.L., Corbetta, M., 2009. Transcranial magnetic stimulation
599 of the human frontal eye field. *J. Neurosci.* 29, 5863–72.

600 <https://doi.org/10.1523/JNEUROSCI.0539-09.2009>

601 Conway, A.R.A., Cowan, N., Bunting, M.F., 2001. The cocktail party phenomenon revisited:
602 The importance of working memory capacity. *Psychon. Bull. Rev.* 8, 331–335.

603 <https://doi.org/10.3758/BF03196169>

604 Corbetta, M., 1998. Frontoparietal cortical networks for directing attention and the eye to visual
605 locations: identical, independent, or overlapping neural systems? *Proc. Natl. Acad. Sci. U.*
606 *S. A.* 95, 831–8. <https://doi.org/10.1073/pnas.95.3.831>

607 Dai, L., Best, V., Shinn-Cunningham, B.G., 2018. Sensorineural hearing loss degrades
608 behavioral and physiological measures of human spatial selective auditory attention. *Proc.*
609 *Natl. Acad. Sci.* 201721226. <https://doi.org/10.1073/pnas.1721226115>

610 Delorme, A., Makeig, S., 2004. EEGLAB: an open source toolbox for analysis of single-trial
611 EEG dynamics including independent component analysis. *J. Neurosci. Methods* 134, 9–21.
612 <https://doi.org/10.1016/j.jneumeth.2003.10.009>

613 Delorme, A., Sejnowski, T., Makeig, S., 2007. Enhanced detection of artifacts in EEG data using
614 higher-order statistics and independent component analysis. *Neuroimage* 34, 1443–1449.
615 <https://doi.org/10.1016/j.neuroimage.2006.11.004>

616 Elhilali, M., Xiang, J., Shamma, S.A., Simon, J.Z., 2009. Interaction between Attention and
617 Bottom-Up Saliency Mediates the Representation of Foreground and Background in an
618 Auditory Scene. *PLoS Biol.* 7, e1000129. <https://doi.org/10.1371/journal.pbio.1000129>

619 Foster, J.J., Sutterer, D.W., Serences, J.T., Vogel, E.K., Awh, E., 2016. The topography of alpha-
620 band activity tracks the content of spatial working memory. *J. Neurophysiol.* 115, 168–177.
621 <https://doi.org/10.1152/jn.00860.2015>

622 Foxe, J.J., Snyder, A.C., 2011. The Role of Alpha-Band Brain Oscillations as a Sensory
623 Suppression Mechanism during Selective Attention. *Front. Psychol.* 2.
624 <https://doi.org/10.3389/fpsyg.2011.00154>

625 Frey, J.N., Mainy, N., Lachaux, J.-P., Muller, N., Bertrand, O., Weisz, N., 2014. Selective
626 Modulation of Auditory Cortical Alpha Activity in an Audiovisual Spatial Attention Task.

627 J. Neurosci. 34, 6634–6639. <https://doi.org/10.1523/JNEUROSCI.4813-13.2014>

628 Haegens, S., Cousijn, H., Wallis, G., Harrison, P.J., Nobre, A.C., 2014. Inter- and intra-
629 individual variability in alpha peak frequency. Neuroimage 92, 46–55.
630 <https://doi.org/10.1016/j.neuroimage.2014.01.049>

631 Haegens, S., Handel, B.F., Jensen, O., 2011. Top-Down Controlled Alpha Band Activity in
632 Somatosensory Areas Determines Behavioral Performance in a Discrimination Task. J.
633 Neurosci. 31, 5197–5204. <https://doi.org/10.1523/JNEUROSCI.5199-10.2011>

634 Hartmann, T., Schlee, W., Weisz, N., 2012. It's only in your head: Expectancy of aversive
635 auditory stimulation modulates stimulus-induced auditory cortical alpha desynchronization.
636 Neuroimage 60, 170–178. <https://doi.org/10.1016/J.NEUROIMAGE.2011.12.034>

637 He, B.J., Snyder, A.Z., Vincent, J.L., Epstein, A., Shulman, G.L., Corbetta, M., 2007.
638 Breakdown of Functional Connectivity in Frontoparietal Networks Underlies Behavioral
639 Deficits in Spatial Neglect. Neuron 53, 905–918.
640 <https://doi.org/10.1016/j.neuron.2007.02.013>

641 Heilman, K.M., Abell, T.V.D., 1980. Right hemisphere dominance for attention: The mechanism
642 underlying hemispheric asymmetries of inattention (neglect). Neurology 30, 327–327.
643 <https://doi.org/10.1212/WNL.30.3.327>

644 Huang, S., Chang, W.T., Belliveau, J.W., Hämäläinen, M., Ahveninen, J., 2014. Lateralized
645 parietotemporal oscillatory phase synchronization during auditory selective attention.
646 Neuroimage 86, 461–469. <https://doi.org/10.1016/j.neuroimage.2013.10.043>

647 Ikkai, A., Dandekar, S., Curtis, C.E., 2016. Lateralization in Alpha-Band Oscillations Predicts
648 the Locus and Spatial Distribution of Attention. PLoS One 11, e0154796.
649 <https://doi.org/10.1371/journal.pone.0154796>

650 Jensen, O., Mazaheri, A., 2010. Shaping Functional Architecture by Oscillatory Alpha Activity:
651 Gating by Inhibition. *Front. Hum. Neurosci.* 4, 186.
652 <https://doi.org/10.3389/fnhum.2010.00186>

653 Kaiser, J., Lutzenberger, W., Preissl, H., Ackermann, H., Birbaumer, N., 2000. Right-
654 Hemisphere Dominance for the Processing of Sound-Source Lateralization.

655 Kelly, S.P., Lalor, E.C., Reilly, R.B., Foxe, J.J., 2006. Increases in Alpha Oscillatory Power
656 Reflect an Active Retinotopic Mechanism for Distracter Suppression During Sustained
657 Visuospatial Attention. *J. Neurophysiol.* 95, 3844–3851.
658 <https://doi.org/10.1152/jn.01234.2005>

659 Kidd, G., Mason, C.R., Gallun, F.J., 2005. Combining energetic and informational masking for
660 speech identification. *J. Acoust. Soc. Am.* 118, 982–992. <https://doi.org/10.1121/1.1953167>

661 Klatt, L.I., Getzmann, S., Wascher, E., Schneider, D., 2018. The contribution of selective spatial
662 attention to sound detection and sound localization: Evidence from event-related potentials
663 and lateralized alpha oscillations. *Biol. Psychol.* 138, 133–145.
664 <https://doi.org/10.1016/j.biopsych.2018.08.019>

665 Klimesch, W., 2012. Alpha-band oscillations, attention, and controlled access to stored
666 information. *Trends Cogn. Sci.* 16, 606–617. <https://doi.org/10.1016/J.TICS.2012.10.007>

667 Klimesch, W., 1999. EEG alpha and theta oscillations reflect cognitive and memory
668 performance: a review and analysis. *Brain Res. Rev.* 29, 169–195.
669 [https://doi.org/10.1016/S0165-0173\(98\)00056-3](https://doi.org/10.1016/S0165-0173(98)00056-3)

670 Klimesch, W., Sauseng, P., Hanslmayr, S., 2007. EEG alpha oscillations: The
671 inhibition{\textendash}timing hypothesis. *Brain Res. Rev.* 53, 63–88.
672 <https://doi.org/10.1016/j.brainresrev.2006.06.003>

673 Knecht, S., 2000. Handedness and hemispheric language dominance in healthy humans. *Brain*
674 123, 2512–2518. <https://doi.org/10.1093/brain/123.12.2512>

675 Kong, L., Michalka, S.W., Rosen, M.L., Sheremata, S.L., Swisher, J.D., Shinn-Cunningham,
676 B.G., Somers, D.C., 2014. Auditory Spatial Attention Representations in the Human
677 Cerebral Cortex. *Cereb. Cortex* 24, 773–784. <https://doi.org/10.1093/cercor/bhs359>

678 Llanos, C., Rodriguez, M., Rodriguez-sabate, C., Morales, I., Sabate, M., 2013.
679 Neuropsychologia Mu-rhythm changes during the planning of motor and motor.
680 Neuropsychologia 1–8. <https://doi.org/10.1016/j.neuropsychologia.2013.02.008>

681 Mesulam, M.-M., 1999. Spatial attention and neglect: parietal, frontal and cingulate
682 contributions to the mental representation and attentional targeting of salient extrapersonal
683 events. *Philos. Trans. R. Soc. London. Ser. B Biol. Sci.* 354, 1325–1346.
684 <https://doi.org/10.1098/rstb.1999.0482>

685 Michalka, S.W., Rosen, M.L., Kong, L., Shinn-Cunningham, B.G., Somers, D.C., 2016.
686 Auditory Spatial Coding Flexibly Recruits Anterior, but Not Posterior, Visuotopic Parietal
687 Cortex. *Cereb. Cortex* 26, 1302–1308. <https://doi.org/10.1093/cercor/bhv303>

688 Murray, M.M., Brunet, D., Michel, C.M., 2008. Topographic ERP Analyses: A Step-by-Step
689 Tutorial Review. *Brain Topogr.* 20, 249–264. <https://doi.org/10.1007/s10548-008-0054-5>

690 Noyce, A., Tobyne, S., Michalka, S., Osher, D., Shinn-Cunningham, B., Somers, D., 2017.
691 Visual, spatial, or visuospatial? Disentangling sensory modality and task demands in frontal
692 cortex. *J. Vis.* 17, 1097. <https://doi.org/10.1167/17.10.1097>

693 O’Sullivan, J.A., Power, A.J., Mesgarani, N., Rajaram, S., Foxe, J.J., Shinn-Cunningham, B.G.,
694 Slaney, M., Shamma, S.A., Lalor, E.C., 2015. Attentional Selection in a Cocktail Party
695 Environment Can Be Decoded from Single-Trial EEG. *Cereb. Cortex* 25, 1697–1706.

696 <https://doi.org/10.1093/cercor/bht355>

697 Okazaki, Y.O., Horschig, J.M., Luther, L., Oostenveld, R., Murakami, I., Jensen, O., 2015. Real-
698 time MEG neurofeedback training of posterior alpha activity modulates subsequent visual
699 detection performance. *Neuroimage* 107, 323–332.

700 <https://doi.org/10.1016/j.neuroimage.2014.12.014>

701 Oldfield, R.C., 1971. The assessment and analysis of handedness: The Edinburgh inventory.
702 *Neuropsychologia* 9, 97–113. [https://doi.org/10.1016/0028-3932\(71\)90067-4](https://doi.org/10.1016/0028-3932(71)90067-4)

703 Oostenveld, R., Fries, P., Maris, E., Schoffelen, J.M., 2011. FieldTrip: Open source software for
704 advanced analysis of MEG, EEG, and invasive electrophysiological data. *Comput. Intell.*
705 *Neurosci.* 2011. <https://doi.org/10.1155/2011/156869>

706 Pfurtscheller, G., Brunner, C., Schlogl, A., Lopes da Silva, F.H., 2006. Mu rhythm
707 (de)synchronization and EEG single-trial classification of different motor imagery tasks.
708 *Neuroimage* 31, 153–159. <https://doi.org/10.1016/j.neuroimage.2005.12.003>

709 Pfurtscheller, G., Neuper, C., Krausz, G., 2000. Functional dissociation of lower and upper
710 frequency mu rhythms in relation to voluntary limb movement. *Clin. Neurophysiol.* 111,
711 1873–9.

712 Pouget, A., Driver, J., 2000. Relating unilateral neglect to the neural coding of space. *Curr. Opin.*
713 *Neurobiol.* [https://doi.org/10.1016/S0959-4388\(00\)00077-5](https://doi.org/10.1016/S0959-4388(00)00077-5)

714 Rihs, T.A., Michel, C.M., Thut, G., 2007. Mechanisms of selective inhibition in visual spatial
715 attention are indexed by ??-band EEG synchronization. *Eur. J. Neurosci.* 25, 603–610.
716 <https://doi.org/10.1111/j.1460-9568.2007.05278.x>

717 Romei, V., Gross, J., Thut, G., 2010. On the Role of Prestimulus Alpha Rhythms over Occipito-
718 Parietal Areas in Visual Input Regulation: Correlation or Causation? *J. Neurosci.* 30, 8692–

719 8697. <https://doi.org/10.1523/JNEUROSCI.0160-10.2010>

720 Sabate, M., Llanos, C., Enriquez, E., Rodriguez, M., 2012. Clinical Neurophysiology Mu rhythm
721 , visual processing and motor control. *Clin. Neurophysiol.* 123, 550–557.

722 <https://doi.org/10.1016/j.clinph.2011.07.034>

723 Samaha, J., Bauer, P., Cimaroli, S., Postle, B.R., 2015. Top-down control of the phase of alpha-
724 band oscillations as a mechanism for temporal prediction. *Proc. Natl. Acad. Sci. U. S. A.*
725 112, 8439–8444. <https://doi.org/10.1073/pnas.1503686112>

726 Samaha, J., Gosseries, O., Postle, B.R., 2017. Distinct Oscillatory Frequencies Underlie
727 Excitability of Human Occipital and Parietal Cortex. *J. Neurosci.* 37, 2824–2833.
728 <https://doi.org/10.1523/JNEUROSCI.3413-16.2017>

729 Samaha, J., Sprague, T.C., Postle, B.R., 2016. Decoding and Reconstructing the Focus of Spatial
730 Attention from the Topography of Alpha-band Oscillations. *J. Cogn. Neurosci.* 28, 1090–
731 1097. https://doi.org/10.1162/jocn_a_00955

732 Sauseng, P., Klimesch, W., Stadler, W., Schabus, M., Doppelmayr, M., Hanslmayr, S., Gruber,
733 W.R., Birbaumer, N., 2005. A shift of visual spatial attention is selectively associated with
734 human EEG alpha activity. *Eur. J. Neurosci.* 22, 2917–2926. [https://doi.org/10.1111/j.1460-9568.2005.04482.x](https://doi.org/10.1111/j.1460-
735 9568.2005.04482.x)

736 Saygin, A.P., Sereno, M.I., 2008. Retinotopy and attention in human occipital, temporal, parietal,
737 and frontal cortex. *Cereb. Cortex* 18, 2158–2168. <https://doi.org/10.1093/cercor/bhm242>

738 Schonwiesner, M., Krumbholz, K., Rubsamen, R., Fink, G.R., von Cramon, D.Y., 2006.
739 Hemispheric Asymmetry for Auditory Processing in the Human Auditory Brain Stem,
740 Thalamus, and Cortex. *Cereb. Cortex* 17, 492–499. <https://doi.org/10.1093/cercor/bhj165>

741 Sereno, M.I., Pitzalis, S., Martinez, A., 2001. Mapping of contralateral space in retinotopic

742 coordinates by a parietal cortical area in humans. *Science* (80-). 294, 1350–1354.

743 <https://doi.org/10.1126/science.1063695>

744 Shinn-Cunningham, B.G., 2008. Object-based auditory and visual attention. *Trends Cogn. Sci.*

745 12, 182–186. <https://doi.org/10.1016/j.tics.2008.02.003>

746 Shulman, G.L., Pope, D.L.W., Astafiev, S. V., McAvoy, M.P., Snyder, A.Z., Corbetta, M., 2010.

747 Right Hemisphere Dominance during Spatial Selective Attention and Target Detection

748 Occurs Outside the Dorsal Frontoparietal Network. *J. Neurosci.* 30, 3640–3651.

749 <https://doi.org/10.1523/JNEUROSCI.4085-09.2010>

750 Silver, M.A., Ress, D., Heeger, D.J., 2005. Topographic Maps of Visual Spatial Attention in

751 Human Parietal Cortex. *J. Neurophysiol.* 94, 1358–1371.

752 <https://doi.org/10.1152/jn.01316.2004>

753 Skrandies, W., 1990. Global field power and topographic similarity. *Brain Topogr.* 3, 137–141.

754 Smith, R.C.G., Price, S.R., 2014. Modelling of Human Low Frequency Sound Localization

755 Acuity Demonstrates Dominance of Spatial Variation of Interaural Time Difference and

756 Suggests Uniform Just-Noticeable Differences in Interaural Time Difference. *PLoS One* 9,

757 e89033. <https://doi.org/10.1371/journal.pone.0089033>

758 Snyder, J.S., Large, E.W., 2005. Gamma-band activity reflects the metric structure of rhythmic

759 tone sequences. *Cogn. Brain Res.* 24, 117–126.

760 <https://doi.org/10.1016/j.cogbrainres.2004.12.014>

761 Strauß, A., Wöstmann, M., Obleser, J., 2014. Cortical alpha oscillations as a tool for auditory

762 selective inhibition. *Front. Hum. Neurosci.* 8, 1–7.

763 <https://doi.org/10.3389/fnhum.2014.00350>

764 Teshiba, T.M., Ling, J., Ruhl, D.A., Bedrick, B.S., Peña, A., Mayer, A.R., 2013. Evoked and

765 Intrinsic Asymmetries during Auditory Attention: Implications for the Contralateral and
766 Neglect Models of Functioning. *Cereb. Cortex* 23, 560–569.
767 <https://doi.org/10.1093/cercor/bhs039>

768 Thut, G., Nietzel, A., Brandt, S.A., Pascual-Leone, A., 2006. Alpha-Band
769 Electroencephalographic Activity over Occipital Cortex Indexes Visuospatial Attention
770 Bias and Predicts Visual Target Detection. *J. Neurosci.* 26, 9494–9502.
771 <https://doi.org/10.1523/JNEUROSCI.0875-06.2006>

772 Tobyne, S.M., Somers, D.C., Brissenden, J.A., Michalka, S.W., Noyce, A.L., Osher, D.E., 2018.
773 Prediction of individualized task activation in sensory modality-selective frontal cortex with
774 ‘connectome fingerprinting.’ *Neuroimage* 183, 173–185.
775 <https://doi.org/10.1016/j.neuroimage.2018.08.007>

776 Tune, S., Wöstmann, M., Obleser, J., 2018. Probing the limits of alpha power lateralisation as a
777 neural marker of selective attention in middle-aged and older listeners. *Eur. J. Neurosci.* 48,
778 2537–2550. <https://doi.org/10.1111/ejn.13862>

779 van Gerven, M., Jensen, O., 2009. Attention modulations of posterior alpha as a control signal
780 for two-dimensional brain–computer interfaces. *J. Neurosci. Methods* 179, 78–84.
781 <https://doi.org/10.1016/J.JNEUMETH.2009.01.016>

782 Weisz, N., Müller, N., Jatzev, S., Bertrand, O., 2014. Oscillatory alpha modulations in right
783 auditory regions reflect the validity of acoustic cues in an auditory spatial attention task.
784 *Cereb. Cortex* 24, 2579–2590. <https://doi.org/10.1093/cercor/bht113>

785 Wightman, F.L., Kistler, D.J., 1992. The dominant role of low-frequency interaural time
786 differences in sound localization. *J. Acoust. Soc. Am.* 91, 1648–1661.
787 <https://doi.org/10.1121/1.402445>

788 Wolpaw, J.R., Birbaumer, N., McFarland, D.J., Pfurtscheller, G., Vaughan, T.M., 2002. Brain–
789 computer interfaces for communication and control. *Clin. Neurophysiol.* 113, 767–791.
790 [https://doi.org/10.1016/S1388-2457\(02\)00057-3](https://doi.org/10.1016/S1388-2457(02)00057-3)

791 Worden, M.S., Foxe, J.J., Wang, N., Simpson, G. V, 2000. Anticipatory biasing of visuospatial
792 attention indexed by retinotopically specific alpha-band electroencephalography increases
793 over occipital cortex. *J. Neurosci.* 20, RC63. <https://doi.org/Rc63>

794 Wöstmann, M., Herrmann, B., Maess, B., Obleser, J., 2016. Spatiotemporal dynamics of
795 auditory attention synchronize with speech. *Proc. Natl. Acad. Sci.* 113, 3873–3878.
796 <https://doi.org/10.1073/pnas.1523357113>

797